GDCh Research Article Angewandte International Edition Chemie www.angewandte.org

How to cite: *Angew. Chem. Int. Ed.* **2024**, *63*, e202405823
doi.org/10.1002/anie.202405823

VIP Antifungal Therapeutics Very Important Paper

Broad Protection against Invasive Fungal Disease from a Nanobody Targeting the Active Site of Fungal β-1,3-Glucanosyltransferases

Sergio Redrado-Hernández[+], Javier Macías-León[+], Jorge Castro-López, Ana Belén Sanz, Elena Dolader, Maykel Arias, Andrés Manuel González-Ramírez, David Sánchez-Navarro, Yuliya Petryk, Vladimír Farkaš, Cécile Vincke, Serge Muyldermans, Irene García-Barbazán, Celia del Agua, Oscar Zaragoza, Javier Arroyo, Julián Pardo, Eva M. Gálvez,* and Ramon Hurtado-Guerrero**

Abstract: Invasive fungal disease accounts for about 3.8 million deaths annually, an unacceptable rate that urgently prompts the discovery of new knowledge-driven treatments. We report the use of camelid single-domain nanobodies (Nbs) against fungal β-1,3-glucanosyltransferases (Gel) involved in β-1,3-glucan transglycosylation. Crystal structures of two Nbs with Gel4 from *Aspergillus fumigatus* revealed binding to a dissimilar CBM43 domain and a highly conserved catalytic domain across fungal species, respectively. Anti-Gel4 active site Nb3 showed significant antifungal efficacy in vitro and in vivo prophylactically and therapeutically against different *A. fumigatus* and *Cryptococcus neoformans* isolates, reducing the fungal burden and disease severity, thus significantly improving immunocompromised animal survival. Notably, *C. deneoformans* (serotype D) strains were more susceptible to Nb3 and genetic *Gel* deletion than *C. neoformans* (serotype A) strains, indicating a key role for β-1,3-glucan remodelling in *C. deneoformans* survival. These findings add new insight about the role of β-1,3-glucan in fungal biology and demonstrate the potential of nanobodies in targeting fungal enzymes to combat invasive fungal diseases.

Introduction

Over 300 million people suffer fungal infections each year, and up to about 3.8 million people, primarily immunocompromised patients, die annually of invasive fungal diseases[1] reaching more deaths per year than HIV, tuberculosis, or malaria.[2] Some of these diseases, such as chronic pulmonary/invasive aspergillosis and meningoencephalitis, caused by *Aspergillus fumigatus* and *Cryptococcus neoformans*,

[*] S. Redrado-Hernández,[+] E. M. Gálvez
Instituto de Carboquímica ICB-CSIC, 50018 Zaragoza, Spain
E-mail: eva@icb.csic.es

S. Redrado-Hernández,[+] M. Arias, O. Zaragoza, J. Pardo, E. M. Gálvez
Center for Biomedical Research in Network in Infectious Diseases (CIBERINFEC), Health Institute Carlos III, 28029 Madrid, Spain
E-mail: pardojim@unizar.es

J. Macías-León,[+] J. Castro-López, A. M. González-Ramírez, D. Sánchez-Navarro, R. Hurtado-Guerrero
Institute of Biocomputation and Physics of Complex Systems (BIFI), University of Zaragoza, Mariano Esquillor s/n, Campus Rio Ebro, Edificio I + D, 50018 Zaragoza, Spain
E-mail: rhurtado@bifi.es

A. Belén Sanz, Y. Petryk, J. Arroyo
Departamento de Microbiología y Parasitología, Facultad de Farmacia, Universidad Complutense de Madrid, 28040, Madrid, Spain

E. Dolader, M. Arias, J. Pardo
Department of Microbiology, Pediatry, Radiology and Public Health, University of Zaragoza, 50009 Zaragoza, Spain

E. Dolader, M. Arias, C. del Agua, J. Pardo
Aragón Health Research Institute (IIS Aragón), Biomedical Research Centre of Aragón (CIBA), 50009 Zaragoza, Spain

V. Farkaš
Department of Glycobiology, Institute of Chemistry, Center for Glycomics, Slovak Academy of Sciences, 84538, Bratislava, Slovakia

C. Vincke, S. Muyldermans
Laboratory of Cellular and Molecular Immunology, Vrije Universiteit Brussel, 1050 Brussels, Belgium

I. García-Barbazán, O. Zaragoza
Mycology Reference Laboratory. National Centre for Microbiology. Health Institute Carlos III28220, Majadahonda, Madrid and Spain

C. del Agua
Department of Pathology, Hospital Clínico Universitario Lozano Blesa, IIS-Aragón, 50009 Zaragoza, Spain

R. Hurtado-Guerrero
Fundación ARAID, 50018 Zaragoza, Spain

R. Hurtado-Guerrero
Copenhagen Center for Glycomics, Department of Cellular and Molecular Medicine, University of Copenhagen, DK-2200 Copenhagen, Denmark

[+] These authors contributed equally: Javier Macías-León and Sergio Redrado-Hernández

respectively, account for up to about 2.2 million deaths annually,[1] further highlighting the significant clinical impact of fungi. Treatments for invasive fungi are mainly limited to polyenes, azoles, and echinocandins.[3] However, the emerging and frequent resistance to current agents,[4] and their toxicity prompts the development of new therapies to combat these infections. This is exemplified by the recent clinical impact and concern caused by *Candida auris*, which has long-term viability outside the human body, and resistance to commonly used antifungals.[5]

Echinocandins, with caspofungin (CSF) as the prototype, bind the fungal β-1,3-glucan synthase (β-1,3-GS) catalytic subunit inhibiting the biosynthesis of β-1,3-glucan.[6] β-1,3-glucan is further modified by cell wall GPI-anchored β-1,3-glucanosyltransferases with elongating and branching activities.[7] These enzymes are known to be involved in the crosslinking of cell wall polysaccharides,[7] which is necessary to ensure cell wall remodeling.[8] They are classified within the GH72[9] family because they share the GH72 catalytic domain, followed by a linker region, but exhibit variations in their C-terminal regions.[10]

Fungi possess a set of β-1,3-glucanosyltransferases, but even with enzymatic redundancy, the elimination of the *GEL4* gene (7 different genes in total) results in non-viable *A. fumigatus*.[10a] Additionally, the loss of either *PHR1* or *PHR2* genes (5 in total) diminishes *C. albicans* virulence.[10b,11] Thus, these critical enzymes constitute promising drug targets for fungal infections.

The use of monoclonal antibodies (mAbs) targeting components of the cell wall has been proposed as potential antifungal therapies against candidiasis, aspergillosis and cryptococcosis.[12] Recently, a combination of one of these antibodies against β-1,3-glucan and fluconazole (FCZ) has also been suggested as an antifungal therapy.[13] However, other types of antibodies, namely camelid-derived antigen-binding variable domains (VHHs or nanobodies, Nbs), have not been explored as antifungal drugs, despite being valuable therapeutics for other diseases.[14] Nbs have emerged as a distinct Ab class due to their low production cost, high solubility, low immunogenicity, and small size, allowing them to reach tissues like the brain, which are more restricted for common antibodies, and especially their ability to recognise dynamic and hidden epitopes.[15] We present a family of Nbs that target Gel4, characterise the binding and inhibition mechanism of these Nbs, and demonstrate the protective effect of one of these Nbs in two animal models of invasive fungal infections.

Results and Discussion

Isolation of *A. fumigatus* Gel4-Directed Nbs

Nbs were obtained after immunizing a llama with *A. fumigatus* deglycosylated Gel4 (dGel4). The deglycosylation of Gel4 was achieved using Endoglycosidase H (EndoH), as detailed in the Supporting Information. dGel4 crossreactive Nbs were isolated using phage display, rendering 8 Nbs grouped in 3 families based on the nature of their H3-sequence (see Methods and Figure S1). Nb2/4/5/6/17/32, Nb3, and Nb22 belonged to families 1, 2, and 3, respectively. All Nbs were expressed in *E. coli* and purified by nickel-immobilised metal affinity chromatography (Figure S2A). The glycosylated Gel4 (gGel4) was expressed in *P. pastoris* and both gGel4 and dGel4 behaved as a monomer under gel filtration chromatography (Figure S2B). The binding affinities of these 8 Nbs against gGel4 and dGel4 were evaluated by isothermal titration calorimetry (ITC; Figure 1A and Figure S3). We also used a control Nb, NbSseK1, which binds to the Arg-glycosyltransferase SseK1 of *Salmonella enterica*.[16] As expected we did not observe any binding of NbSseK1 to dGel4 (Figure S3). All our 8 Nbs exhibited approximately 1:1 binding to either gGel4 or dGel4, with affinity constants in the low and medium nM range (Figure S4 and Table S1). Detailed analysis of the thermodynamic parameters of the interaction showed that the binding of Nb3 to either enzymatic form and Nb6 to gGel4 were largely entropy-driven ($-T\Delta S$). At the same time, the other Nbs were favored by a gain in enthalpy (ΔH), suggesting distinct interaction behaviours (see the structural analysis below for a detailed discussion).

Inhibition of Gel4 Enzymatic Activity by the Nbs

To evaluate the inhibitory capacity of the Nbs, the transglycosylase activity of gGel4 was measured in a time-course fluorescent assay in the presence of the Nbs using laminarin (β-1,3-glucan) as the glucanosyl donor and sulphorhodamine-labeled laminarihexaose as the acceptor substrate.[17] A 5-fold molar ratio of Nbs over gGel4 (5:1 ratio) showed that all Nbs inhibited gGel4 activity (Figure 1B-left panel, and Figure S5A). At a lower molar ratio (2:1), Nb2, Nb3, Nb4, and Nb6 were the most potent ones, followed to a lesser extent by Nb22 and Nb17 (Figure 1B-right panel and Figure 1C). The control NbSseK1 did not show any inhibition on Gel4. Since Nb2, Nb4, and Nb6 all belonged to the same family 1 (Figure S1), Nb4 was selected for further enzymatic studies. To assess the impact of protein glycosylation on Gel4 inhibition, we compared the IC_{50} values for Nb3 and Nb4 against both gGel4 and dGel4 proteins, finding no significant differences in the inhibition of gGel4 or dGel4 by either Nb3 or Nb4 (Figure S5B). We also assessed the activity of other $GH72^{+}$ subfamily members, specifically Phr1 and Phr2 from *C. albicans*, as well as Gas1 and Gas2 from *S. cerevisiae*, in the presence of Nb3 and Nb4. *A. fumigatus* Gel1 and Gel2, classified within the $GH72^{-}$ subfamily, were excluded from the experiment due to their distinct dissimilarity to Gel4, chiefly characterised by the absence of the CBM43 domain. In comparison to Nb3′s potent inhibition of Gel4 activity reaching up to about 100 % inhibition at a 5:1 ratio, Nb3 moderately inhibited Gas2 at the same ratio (5:1), and inhibited poorly Phr1/Phr2 (200:1 ratio was required to see a significant inhibition). In contrast, Nb4 only inhibited Phr2 at a high concentration (200:1; Figure S5C,D). These results suggest that Nb3 and Nb4 are fairly selective inhibitors of Gel4, although Nb3 can

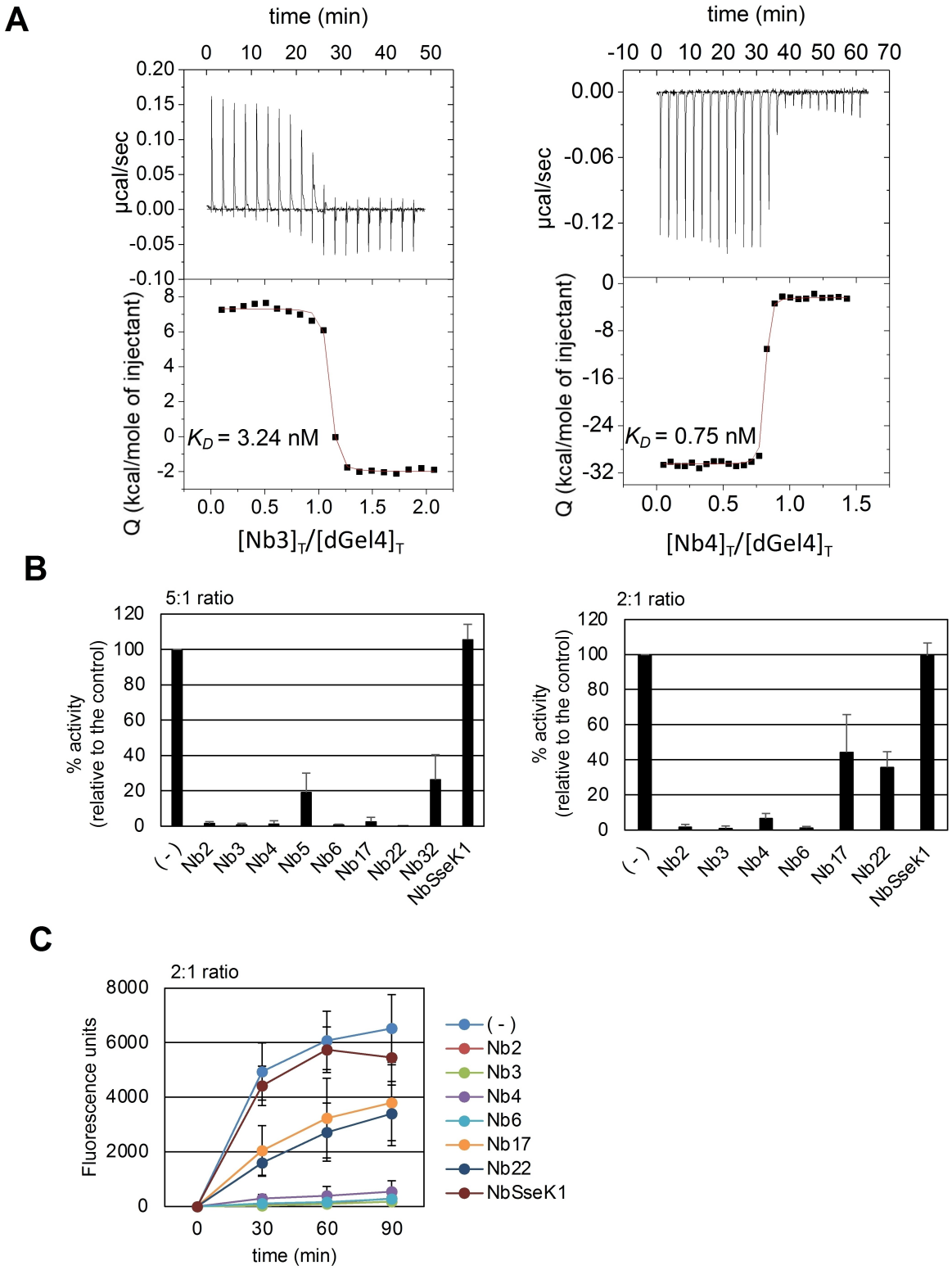

Figure 1. Biophysical characterization of Nbs. A) ITC data for the binding of Nb3 and Nb4 to dGel4. Top: raw thermogram (thermal power versus time). Bottom: binding isotherm (normalised heats versus molar ratio). B) Inhibition of β-(1,3)-glucanosyltransglycosylase enzymatic activity of gGel4 by the Nbs at 5-fold (left panel) and 2-fold (right panel) molar excess. The inhibitory effect of Nbs is expressed as a percentage of gGel4 enzymatic activity in the presence of the Nbs after reaction for 30 min relative to the control (absence of Nb). C) Inhibition time-course of gGel4 enzymatic activity by the indicated Nbs at 2-fold molar excess. NbSseK1 against the *Salmonella enterica* SseK1 protein unrelated to Gel4 was used as a negative control.[25] Data are shown as mean ± standard deviation (SD) from at least three independent experiments.

inhibit other Gel4 orthologs more broadly at higher concentrations.

Structural Basis of Nbs Interactions with Gel4

To elucidate the molecular basis of Gel4 inhibition by the most potent Nbs, we determined the crystal structures of dGel4 complexed to Nb3 and Nb4 at 2.05-Å and 1.90-Å resolution, respectively (Figure 2A,B and Table S2). The structure of dGel4, as described before for Gas2 crystal structures,[18] shows a compact structure with the typical $(\beta/\alpha)_8$ catalytic core and the cysteine-rich CBM43 domain located at the N- and C-terminal regions, respectively. While Nb4 binds to the CBM43 domain burying a Gel4 surface area (SA) of 3,870 $Å^2$, Nb3 binds to a shallow active site located in the catalytic domain, burying a larger SA of 4,860 $Å^2$. Particularly, Nb3 occupies the −6 to −1 and +1 to +5 sugar-binding subsites, impeding binding to β-1,3-glucan and in turn transglycosylation (Figure 2A,C). These data suggest that our Nbs might adopt at least two different binding modes inhibiting Gel4. Note also that the Gel4 catalytic domain residues interacting with Nb3 are more conserved across orthologs than the CBM43 domain residues interacting with Nb4 (Figure 2A,B; further discussed below), which might explain why Nb3 can also inhibit other Gel4 orthologs (see above).

When comparing the Gas2-laminaripentaose (G5)[18] and dGel4-Nb3 structures, it is clear evident that they share most secondary structure elements and align well (RMSD 1.39 Å on 403 equivalent Cα atoms; Figure 2D and Figure S6). However, RMSDs slightly increase when comparing Gas2-G5 and dGel4-Nb3 complexes with Gel4-Nb4 complex (RMSDs 1.76 Å and 1.56 Å on 398 and 408 Cα atoms), due to conformational changes caused by Nb4 binding to Gel4 in the CBM43 α10/α12/β14 and loops (Figure 2D).

In the dGel4-Nb3/4 interfaces, the H1, H2, and H3 loops play a pivotal role in dGel4 recognition (Figures S7 and S8). Nb3 primarily interacts with conserved residues in the catalytic domain (9/16 residues are completely conserved with Gel4 orthologs; Figure 2E, Figure S9 and Table S3), including critical ones like N158/E159/E261 and Y230/Y293/Y302.[18–19] Conversely, Nb4 interacts with specific residues in the Gel4 CBM43 domain, with fewer conserved residues between Gel4 orthologs (Figure 2E, Figure S10, and Table S3). Most of these interactions involve hydrogen bonds and salt bridges mainly through side chains (Table S3). However, hydrophobic interactions were also present, though these were in the minority in the dGel4-Nb3 complex. Nb3′s residues interacting with dGel4 differ from other Nbs, while Nb4 shares mostly conserved residues with family 1 Nbs (Nbs2/5/6/17/32), suggesting similar binding modes. Nb22, which belongs to another family, may adopt a unique binding mode. The distinct thermodynamic profile of Nb3 likely results from the release of many water molecules from Gel4′s active site upon Nb3 binding, which could favor desolvation entropy. However, this hypothesis will require further experimental validation. The crystal structure of Gas2 E176Q, unlike that of dGel4-Nb4 complex, offers clearer evidence because dGel4′s active site is obstructed by another dGel4 from a neighboring asymmetric unit (Figure S11). In Gas2 E176Q structure, numerous water molecules occupy the catalytic binding site, contrasting with Nb4′s CBM43 binding site.

A CBM43 Phe Residue Interacting with Nb4 Modulates Transglycosylation

A prior study suggested that fungal Gas2′s CBM43 may bind to β-1,3-glucan, yet this remained unconfirmed experimentally.[18] In contrast, plant-derived CBM43 domains were shown to bind β-1,3-glucan.[20] Additionally, the structures of CBM43 domains from Ole e 9[21] and Gas2[18] exhibited significant differences and did not provide molecular-level insights into the interaction of CBM43s with β-1,3-glucan. Nb4 binding to CBM43 and its inhibitory effect suggest CBM43 interacts with β-1,3-glucan and plays a crucial role in transglycosylation. To investigate further, we examined specific aromatic residues, $F394^{Gel4}$ and $Y396^{Gel4}$, that interact with Nb4 (Figure 2E). We also investigated $F415^{Gas2}$, the equivalent residue to $F394^{Gel4}$ (Figure S6). We created Ala mutants for $F394^{Gel4}$, $Y396^{Gel4}$, $F415^{Gas2}$, and the $F415R^{Gas2}$ mutant. Results indicated that $Y396^{Gel4}$ was not essential for transglycosylation, while $F394^{Gel4}$ and $F415^{Gas2}$ played important roles. $F394A^{Gel4}$ reduced activity by about 50 %, and $F415A^{Gas2}$ and $F415R^{Gas2}$ led to approximately 80 % and 97 % activity reductions, respectively (see Figure S12). This suggests CBM43 modulates transglycosylation by interacting with β-1,3-glucan, potentially leading to competition among Nbs in family 1 (Nbs2/4/5/6/17/32) for CBM43 domain association with β-1,3-glucan sugar units.

In vitro Inhibitory Effect of Nb3 on the Growth of Different Fungal Species

Having established the mechanism of Nb3-mediated inhibition of Gel4, we next questioned whether Nb3 could be effective in inhibiting the growth of *C. albicans*, *A. fumigatus* and *C. neoformans* species complex (serotypes A and D) including azole-resistant strains. Although there are no studies of these enzymes in *Cryptococcus spp.*, we performed a BLAST search using the Gel4 catalytic domain against the *C. neoformans* genome, and found only one member in this fungus, which we named hereafter as *Cn*Gel (ca. 41 % identity with Gel4; Figures S9 and S10). Nb3 inhibited *C. albicans* growth very poorly at 37 °C (Figure S13) in agreement with the low inhibitory properties of Nb3 on Phr isoenzymes (Figure S5C). In contrast, Nb3 inhibited *A. fumigatus* growth at 37 °C fairly well in different strains, including the azole-resistant 678715, and strongly inhibited cell growth of *C. deneoformans* strains at 30 °C (former *C. neoformans* serotype D), albeit inhibited poorly growth of *C. neoformans* (serotype A) strains (Figure 3A,C and Table S4). Using NbSseK1 control, no antifungal activity was observed, further confirming that the inhibitory effect of Nb3 was not due to the relatively high doses used.

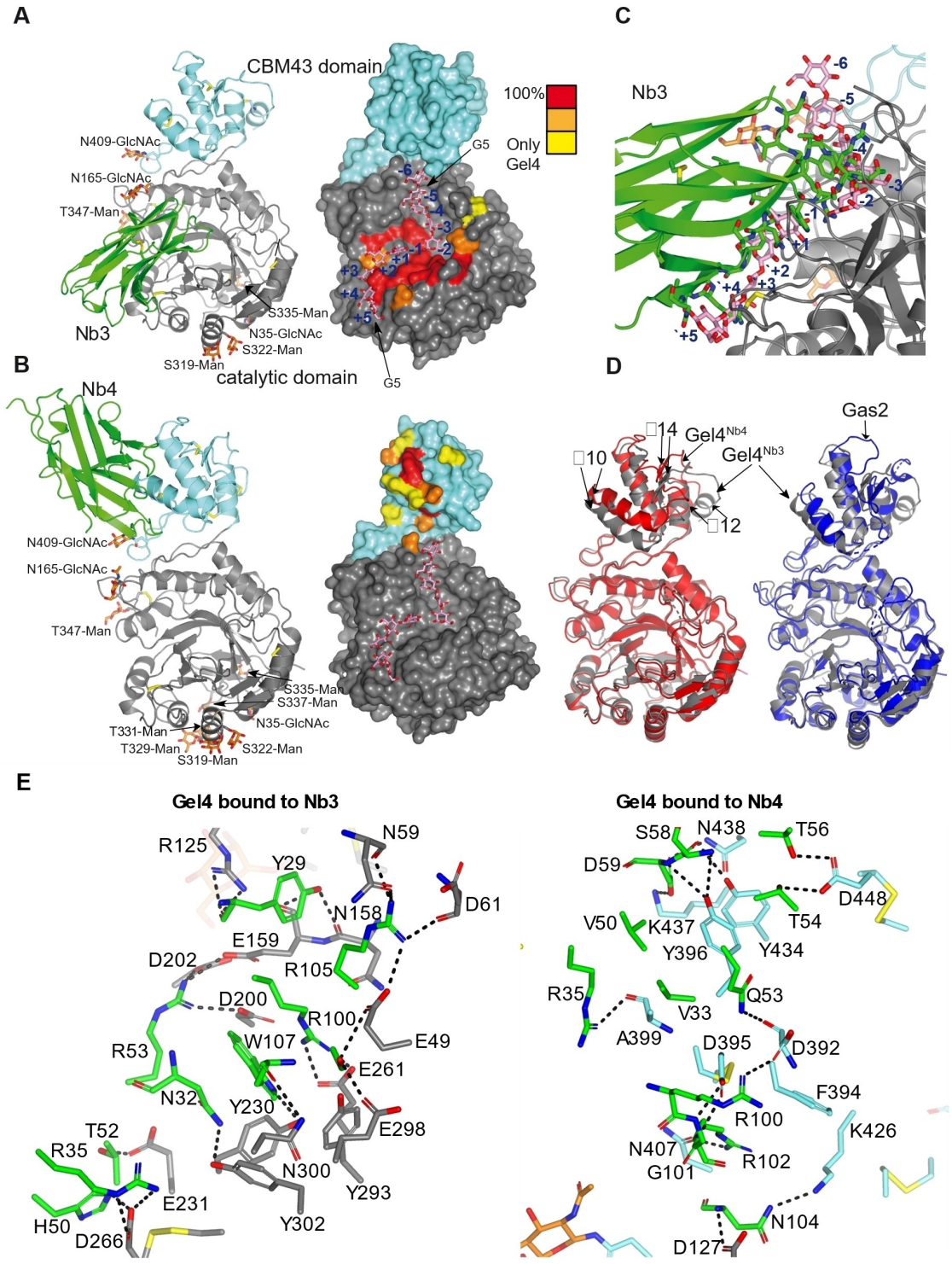

Figure 2. Overall structures of dGel4 complexed to Nb3 and Nb4. A,B) Left: Ribbon structures of dGel4 complexed to Nb3 (top, A) and Nb4 (bottom, B). The catalytic and CBM43 domains and the Nbs are colored grey, aquamarine, and green, respectively; *N*-linked glycans (3 in total) and *O*-linked glycans (7 in total; man stands for mannose) are shown as orange carbon atoms; disulfide bridges are indicated as yellow sulfur atoms. Right: Surface representation of dGel4-Nb3 and dGel4-Nb4 complexes, color-coded by degree of sequence conservation in the interacting regions between Gel4 and Nb3/Nb4. G5 coordinates were obtained from Gas2 complexed to G5 (PDB entry 2W62[18]) and are displayed to indicate the sugar-binding subsites in Gel4. Sugar units are colored as pink carbon atoms. C) Close-up view of the dGel4-Nb3 with G5 to evidence the competitive inhibition mechanism of Nb3. D) Superposition of $dGel4^{Nb3}$ (grey) and $dGel4^{Nb4}$ (red) structures (left panel), and $dGel4^{Nb3}$ and Gas2 (red) structures (right panel). E) Close-up view of the interfaces of dGel4-Nb3 and dGel4-Nb4 complexes. The residues of dGel4 catalytic and CBM43 domain, and Nb3/4, engaged in hydrogen bond and hydrophobic interactions, are depicted as grey, aquamarine, and green carbon atoms, respectively. Hydrogen bonds are shown as dotted black lines.

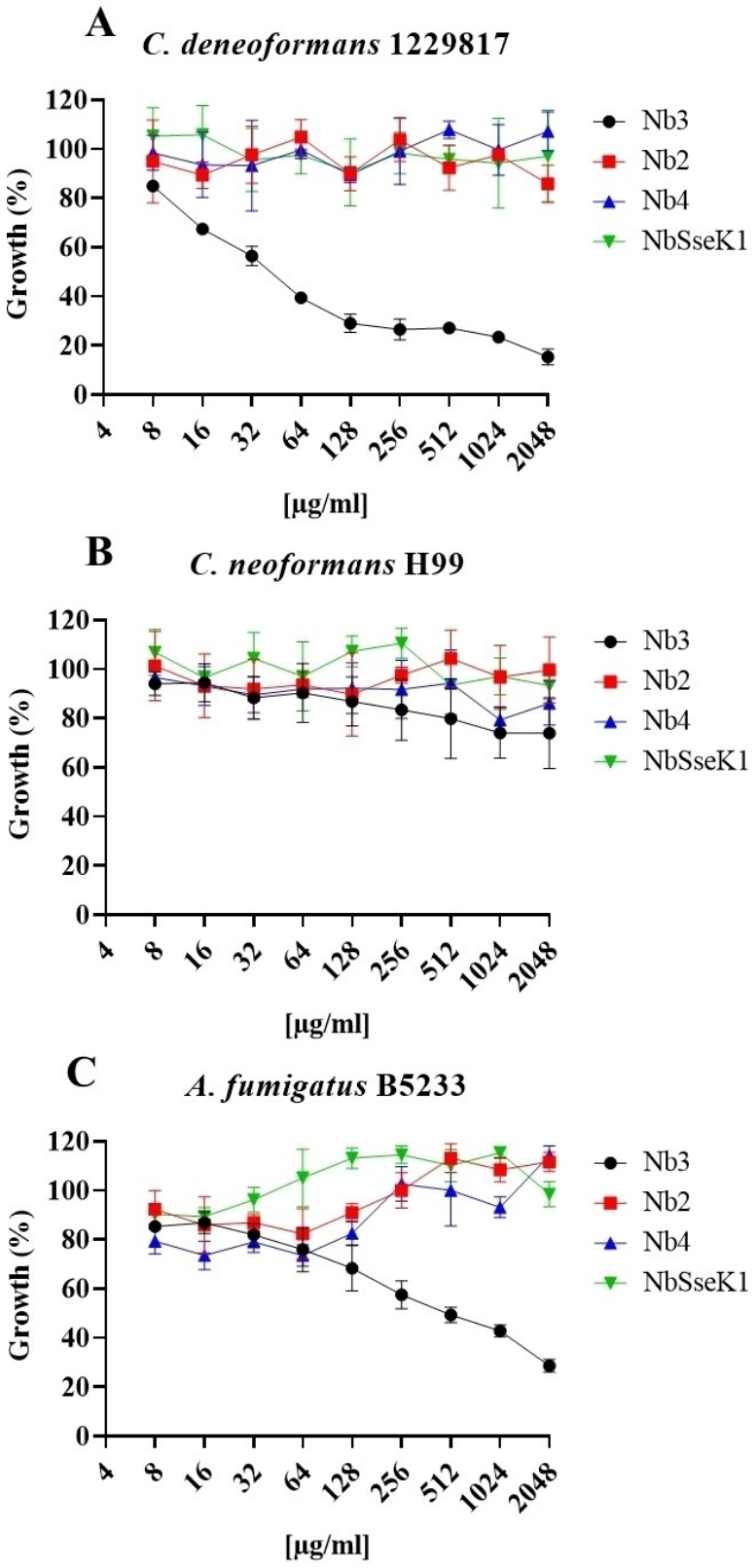

Figure 3. Sensitivity of *C. deneoformans*, *C. neoformans* and *A. fumigatus* to Nb3. The antifungal activity of different concentrations of Nb3, Nb2, Nb4, or NbSseK1 against *C. deneoformans* 1229817 (A), *C. neoformans* H99 (B), and *A. fumigatus* B5233 (C) was measured with XTT reduction assay as described in the Supporting Information. Results are presented as the growth percentage compared to untreated controls. The experiments with *A. fumigatus* and *C. neoformans* species complex were performed at 37 °C and 30 °C, respectively. Data represent the mean and standard deviation of at least three independent experiments.

Furthermore, despite the ability of Nb2 and Nb4 to inhibit Gel4 activity in vitro, they did not exhibit any antifungal activity (further discussed below; Figure 3A,C and Figure S10). To further explain the difference in growth under the presence of Nb3 between *C. neoformans* and *C. deneoformans* strains, we generated a *CnGel* knockout in *C. neoformans* H99 strain (H99 *CnGel−)*, which remained viable and did not present any growth delay, indicating that this enzyme is dispensable for survival in this strain (Supporting Information). Additionally, as expected, none of the Nbs affected H99 *CnGel−* growth (Figure S14). In contrast, using the same disruption strategy, we were not able to obtain *CnGel* mutants in *C. deneoformans* JEC21 strain, suggesting that this enzyme is important for *C. deneoformans* survival, thus supporting the inhibitory growth effect of Nb3 in these strains. To check if differences in growth were caused by differences in *Cn*Gel inhibition depending on the strain, we expressed and purified *Cn*Gel from both strains using *P. pastoris* (Figure S2). When tested, both enzymes were inhibited by Nb3, though at a lower substrate concentration and higher Nb3/*Cn*Gel ratio than the one used for Nb3/Gel4 (Figure S15A). Furthermore, the K_Ds indicated that Nb3 bound worse to the enzymes *Cn*Gel^{H99} (Uniprot ID: J9VZ45) and *Cn*Gel^{JEC21} (Uniprot ID: Q5K6U3) than to Gel4 (ca. 21-fold and ca. 270-fold lower binding than that of Nb3 on gGel4, respectively; Figure S15B). This may explain why Nb3 had a weaker inhibitory effect on both *Cn*Gel enzymes than Gel4.

Effect of the Combination of Nb3 with Antifungal Drugs

Next, we conducted experiments to measure growth inhibition when Nb3 was combined with Nb4, voriconazole (VCZ) or amphotericin B (AMB) for *A. fumigatus* B5233, and Nb3 with Nb4, FCZ or AMB for both *C. neoformans* H99 and *C. deneoformans* 1229817. We first determined the MIC_{50} values for AMB, FCZ, and VCZ against these pathogens, which revealed, as expected, that VCZ was a potent drug against *A. fumigatus* B5233, AMB was also very potent against all tested organisms, and FCZ was a modest inhibitor on both *Cryptococcus* strains (Table S5). Additionally, we included CSF in our experiments, revealing that this drug showed modest inhibitory properties on *A. fumigatus* B5233 and *C. deneoformans* 1229817 and its efficacy was reduced against *C. neoformans* H99 (Table S5). Combined with our results using Nb3, this suggests that the inhibition of β-1,3-glucan synthesis or remodeling is not essential for *C. neoformans* H99 growth, which further stresses the remarkable differences between *Cryptococcus* strains. In fact, *C. deneoformans* B3501 and JEC21 strains showed several cell wall integrity phenotypes, including hypersensitivity to SDS and Congo Red, whereas *C. neoformans* H99 and KN99 strains did not (Figure S16).[22] Next, we analysed potential synergies between Nb3 and antifungal drugs, revealing that only the combination of Nb3 with AMB or, intriguingly, Nb4 in *A. fumigatus* B5233 cultures showed synergy (FICI = 0.378 and 0.063, respectively). Interestingly, additive effects were also observed for Nb3 combined with AMB in *C. neoformans* H99 and *C. deneoformans* 1229817 cultures. Furthermore, the combination of Nb3 with azole drugs showed additive effects in almost all cases (Table S6).

Characterization of Nb3-Mediated Modification of Sugar Composition in *C. neoformans* and *C. deneoformans* Strains

In order to analyse if Nb3 is able to cross the *Cryptococcus* capsule and reach its target, whether it is on the plasma membrane via its GPI anchor (as shown for Gel4[10a] or Phr1[23]) or within the cell wall (as found for Phr1[23] and Gas1/Gas3/Gas5[24]), we performed immunofluorescence confocal microscopy experiments in susceptible and resistant *C. neoformans* and *C. deneoformans* strains. Nb3 crossed the polysaccharide capsule (FITC) in all *C. neoformans* and *C. deneoformans* strains, mainly localizing in the cell wall (calcofluor white) or the outer layer plasma membrane (Figure 4). Therefore, the different susceptibility was unlikely due to an inability to cross the cell capsule and reach its target; this was further supported by similar binding of Nb3 in capsular and acapsular strains derived from B3501 and H99. Furthermore, a fusion protein comprising Nb3-Fc (human IgG1 Fc) displayed very low antifungal activity against the susceptible *C. deneoformans* 1229817 strain, which suggests that the small size of Nb is essential for its antifungal activity against *C. deneoformans* strains in vitro (Figure S17). Note also that no staining was observed when using the H99 *CnGel*-mutant, confirming the specificity of Nb3 binding to *Cn*Gel (Figure 4). A similar result was found when the localization of Nb3 was analysed in *A. fumigatus* hyphae (Figure 4H), showing that Nb3–Cy5 colocalises with calcofluor white staining. This confirms the presence of Nb3 in the *Aspergillus fumigatus* cell wall where Gel4 is located, and, together with *C. neoformans* stainings, supports its specificity for this enzyme.

HPLC analysis of cell wall and capsule extracts indicated that Nb3 significantly decreased the glucose content of *C. neoformans* H99 and *C. deneoformans* 1229817 and B3501 ($p < 0.05$) and increased the mannose content compared to untreated cells (Figure 5A). As expected, no significant changes in the carbohydrate composition were observed between untreated and treated H99 *CnGel-* strains further confirming the specificity of Nb3 for Gel4. In order to confirm these results performed using acid digestions of cell wall, we analysed changes in cell wall composition by analyzing and quantifying calcofluor white fluorescence in fungal cells before and after Nb3 treatment. As shown in Figure 5B–D, it can be observed a clear and significant reduction in the fluorescence intensity after Nb3 treatment indicating a lower binding of calcofluor white to the cell wall glucan, which suggests a reduction of glucan complexity in cell wall as calcofluor white binding positively correlates with glucan amount/complexity as recently shown.[25] While calcofluor white is also known to bind to chitin,[26] the fact that chitin is barely present in *C. neoformans* serotypes[27] suggests that the observed reduction in fluorescence intensity is primarily due to decreased glucan complexity. Altogether the results show that Nb3 affects *C. deneofor-*

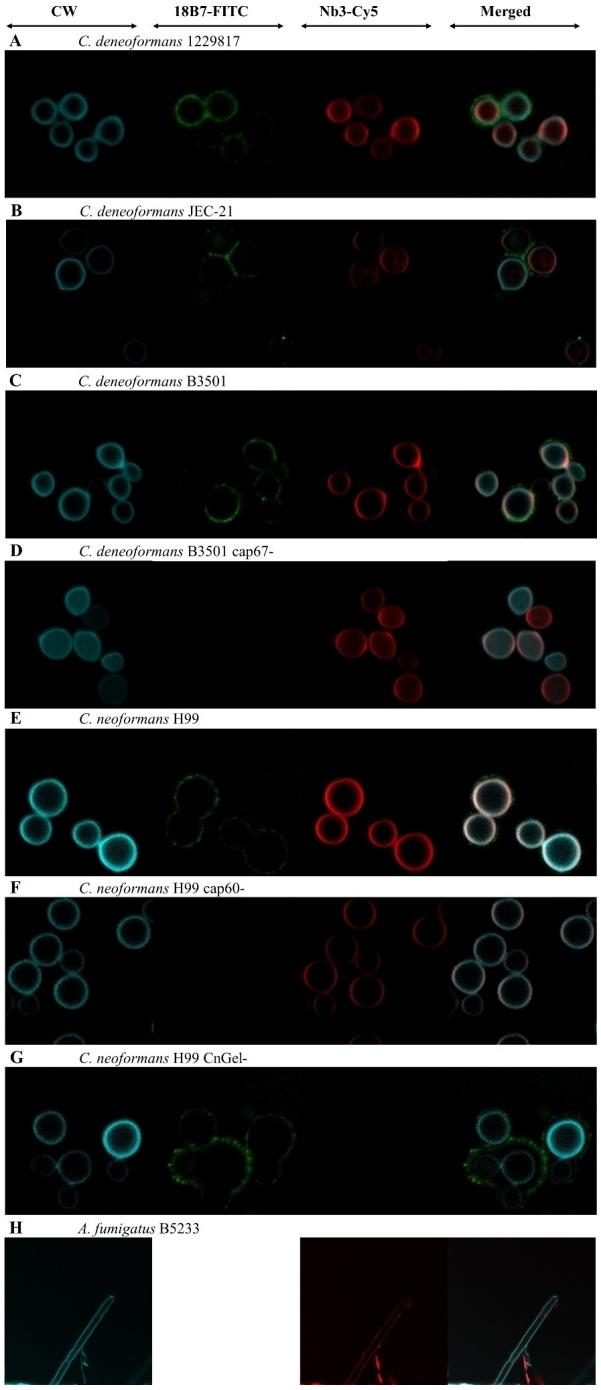

Figure 4. Location of Nb3 in *C. neoformans*, *C. deneoformans and A. fumigatus.* Different *C. neoformans* strains were incubated at room temperature for 15 min with calcofluor white (CW), 18B7-FITC antibody and Nb3-Cy5. The strains employed were *C. deneoformans* 1229817 (A), *C. deneoformans* JEC21 (B), *C. deneoformans* B3501 (C), *C. deneoformans* B3501 *cap67*– (D), *C. neoformans* H99 (E), *C. neoformans* H99 *cap60*– (F), *C. neoformans* H99 *CnGel*– (G) and *A. fumigatus* B5233 (H). The left panels show calcofluor white staining (cyan), which binds to chitin and β-glucans that form the fungal cell wall. Central panels display the locations of the capsule and *Cn*Gel/Gel4 resulting from the recognition of glucuronoxylomannan, a major component of the *Cryptococcus* capsule, and *Cn*Gel/Gel4 by the 18B7-FITC antibody (green) and Nb3–Cy5 (red), respectively. Finally, right panels show merged channels. Images were acquired with a Zeiss LSM 880 (Zeiss, Jena, Germany) confocal microscope.

mans survival by altering cell wall composition, specifically by interacting with *Cn*Gel, and that *C. neoformans* strains can adjust to these changes without compromising growth.

Prophylactic and Therapeutic Treatment of Invasive Aspergillosis and Cryptococcosis with Nb3 shows high in vivo Efficacy in Two Different Animal Models

To assess in vivo protection, we evaluated the efficacy of oral administration of Nb3 on *C. elegans* previously infected with *A. fumigatus* and *C. deneoformans.* Most untreated animals died after 48 h of infection, while Nb3 treatment showed a dose-dependent effect (Figure S18). Then, we selected a dose of 1 mg/mL of Nb3, which resulted in approximately 60 % survival of infected *C. elegans* by both fungi, and compared its effect with other antifungal drugs in a concentration that had been previously found to affect fungal growth without showing toxicity signs in worms (Gehan-Breslow-Wilcoxon test p-value < 0.0001; Figure 6A,B). Nb3 led to similar survival rates to those found for the antifungal drugs. The high Nb3 concentration was required to account for the possibility of Nb3 being partly degraded by the *C. elegans* digestive system. Despite this high concentration, Nb3 was safe in *C. elegans* (Figure S19). Longer incubation times are impossible in this model, as control worms began to die after 72 h due to nutrient restriction, as previously shown.[28]

Next, we evaluated the efficacy of Nb3 as a prophylactic treatment on immunocompromised BALB/c mice infected intranasally (IN) with *A. fumigatus*[29] and *C. deneoformans.*[30] We observed approximately 80 % survival after intraperitoneal (IP) inoculation at doses of 20 and 80 mg/Kg against *C. deneoformans* and *A. fumigatus* infection, respectively (Figure 7A,B). This was further supported by a significant reduction in CFU for *Cryptococcus* infection (Figure 7C). On the contrary, a dose of 40 mg/Kg against *A. fumigatus* infection showed no significant difference compared to the untreated infected mice (Figure 7B). A lower dose of Nb3 (20 mg/Kg) administered IN was sufficient to protect 100 % of mice from death by invasive aspergillosis (Figure 7B). Although Nb2 and Nb4 did not show any antifungal activity in vitro, we analysed the potential antifungal activity of Nb2 in the mouse model to find out whether Nb binding activates host factors that might enhance its activity and contribute to fungal control. However, as expected from in vitro cell cultures, Nb2 did not present any antifungal activity (Fig S20). Given these results and the similarity between Nb2 and Nb4, we did not further test Nb4 in vivo in order to reduce the number of mice used following the guidelines of the ethics committee.

Then we evaluated the Nb3 as a therapeutic treatment. IP administration of Nb3 at 20 mg/Kg significantly improved survival compared to vehicle (PBS)-treated mice in those infected with *C. deneoformans*, rendering more than 60 % mouse survival, while all control mice died after five weeks of infection (Figure 8A). Intranasal administration of Nb3 at 20 mg/Kg led to 80 % of mouse survival (Figure 8B). This efficacy of Nb3 was further supported by the significant

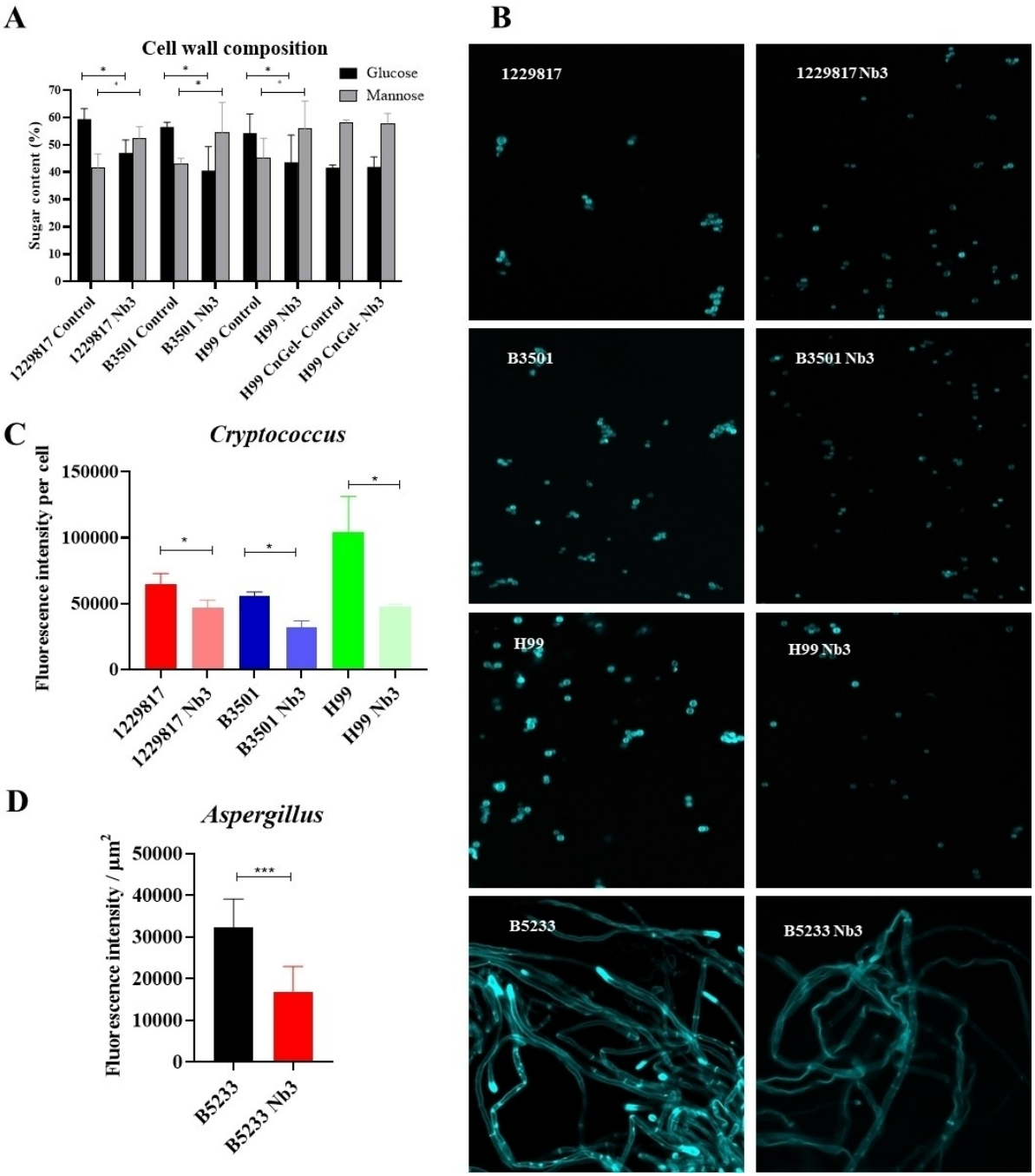

Figure 5. Single sugar profile of *Cryptococcus* cell wall and capsule extracts. A) Single sugar profiles (glucose and mannose) from acid-digested cell wall polysaccharides from 24 h cultures of *C. deneoformans* (1229817 and B3501) and *C. neoformans* (H99) were analysed by HPLC as described in the Supporting Information. Results were analysed by two-way ANOVA with Bonferroni post-test. Data represent the mean and standard deviation of at least three independent experiments. p value < 0.05 (*) for 1229817 control vs. Nb3, B3501 control vs. Nb3 and H99 control vs. Nb3. B) Confocal microscopy images of *C. deneoformans* and *C. neoformans* cells, as well as *A. fumigatus* hyphae, cultured in RPMI 1640 with Nb3 or without Nb3 for 24 h and stained with calcofluor white. The images were captured using a Zeiss LSM 880 confocal microscope (Zeiss, Jena, Germany). C,D) Fluorescence intensity per cell of *C. neoformans* and *C. deneoformans* (C) or per µm^2 of hyphae of *A. fumigatus* (D) previously cultured with Nb3 and stained with calcofluor white. Results were analysed by unpaired t-test. $p < 0.05$ (*) for *C. deneoformans* 1229817 and *C. neoformans* H99 control vs. Nb3, $p < 0.01$ (**) for *C. deneoformans* B3501 control vs. Nb3 and $p < 0.001$ (***) for *A. fumigatus* B5233 control vs Nb3.

reduction of *C. deneoformans* colonization in lungs and brain (Figure 8C–F) as well as by a reduction in the pathology observed in lungs from treated animals in comparison with non-treated controls (Figures 8G and S21). Importantly, tissue homogenates from treated animals showed that Nb3 was able to reach lungs and brain of *C.*

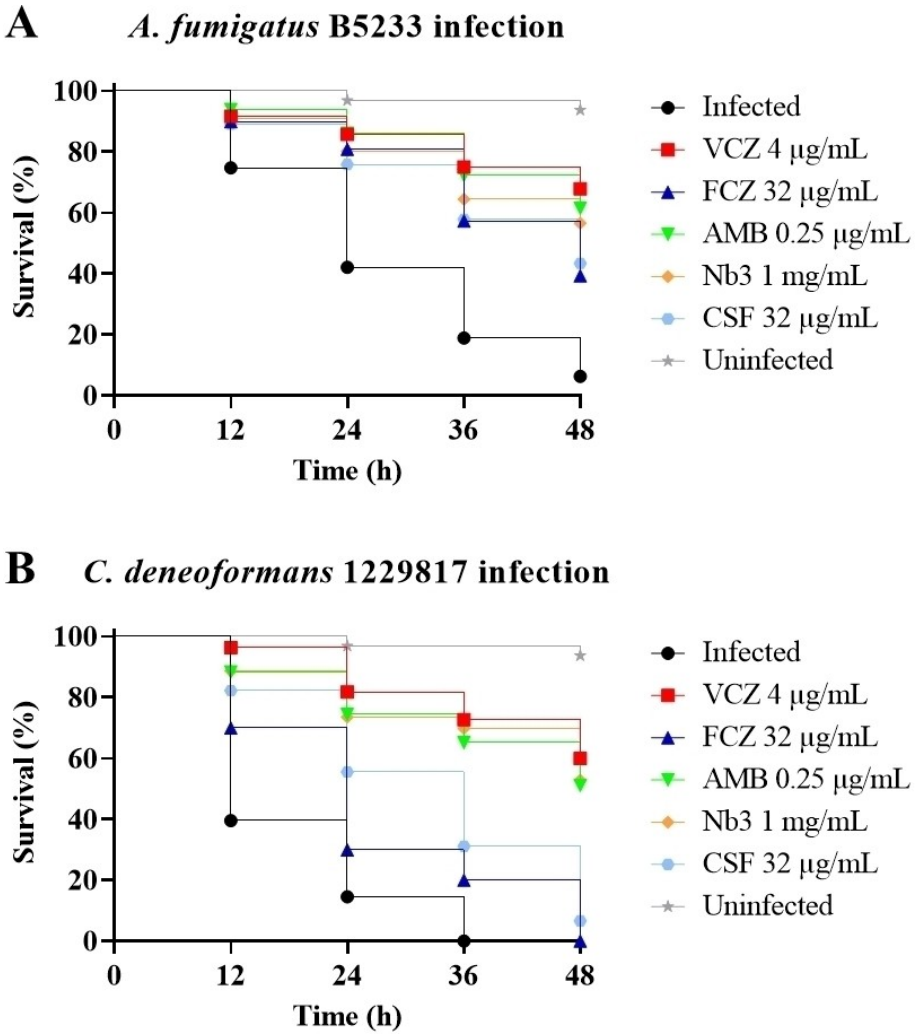

Figure 6. Efficacy of Nb3, VCZ, FCZ, AMB and CSF in a *C. elegans* model of *A. fumigatus* and *C. deneoformans* infection. Survival of L4 larvae of *C. elegans* after infection with *A. fumigatus* B5233 (A; $n=412$) or *C. deneoformans* 1229817 (B; $n=443$) in the absence or presence of 1 mg/mL Nb3, 4 µg/mL VCZ, 32 µg/mL FCZ, 0.25 µg/mL AMB and 32 µg/mL CSF. Experiments were performed in triplicate and the results were analysed using the mantel-Cox test. p value <0.0001 for the comparison between the treated groups and infected groups in both experiments.

deneoformans infected mice (Figure 8H,I), thereby confirming the efficacy of treating both pulmonary and brain infection, which correlates with the increase in mouse survival.

Next, we determined the efficacy of Nb3 administered IN (Figure 9A) or IP (Figure 9B) 24 h after infection in an aspergillosis mouse model. We used a dosage of Nb3 (80 mg/Kg) because the lower doses of 40 mg/Kg used in the prophylactic experiment showed no positive effect on mouse survival (Figure 7B). This dose (80 mg/Kg) improved mouse survival, reaching a statistically significant approximately 80 % (Figure 9B). In contrast, only about 20 % of control mice treated IP with vehicle (PBS) survived (Figure 9B). Additionally, the IN therapeutic administration of a lower dose of our Nb3 at 20 mg/Kg led to a 50 % survival compared to control mice, which all died within the first week of infection (Figure 9A), indicating that this mode of administration may be more beneficial than IP, as it requires lower doses of the drug. These experiments were further validated by a significant decrease in *A. fumigatus* colonization in the lung, as determined by measuring fungal burden in tissue using real-time qPCR (Figure 9C). In addition, the comparison of the histopathologic scores of Nb3-treated and non-treated individuals (Figures 9D and S21) showed a significant improvement in the lungs of Nb3-treated mice.

As shown in vitro, no effect was observed with NbSseK1 in any of the mouse models, although it similarly reached the lungs and brain, confirming the selective antifungal activity of Nb3 (Figure 8A–F). Overall, these results demonstrate the efficacy of Nb3 in both prophylactic and therapeutic treatments of invasive aspergillosis and cryptococcosis.

Discussion and Conclusions

New strategies to tackle invasive fungal infections are critical due to rising mortality and drug resistance. Triazoles,

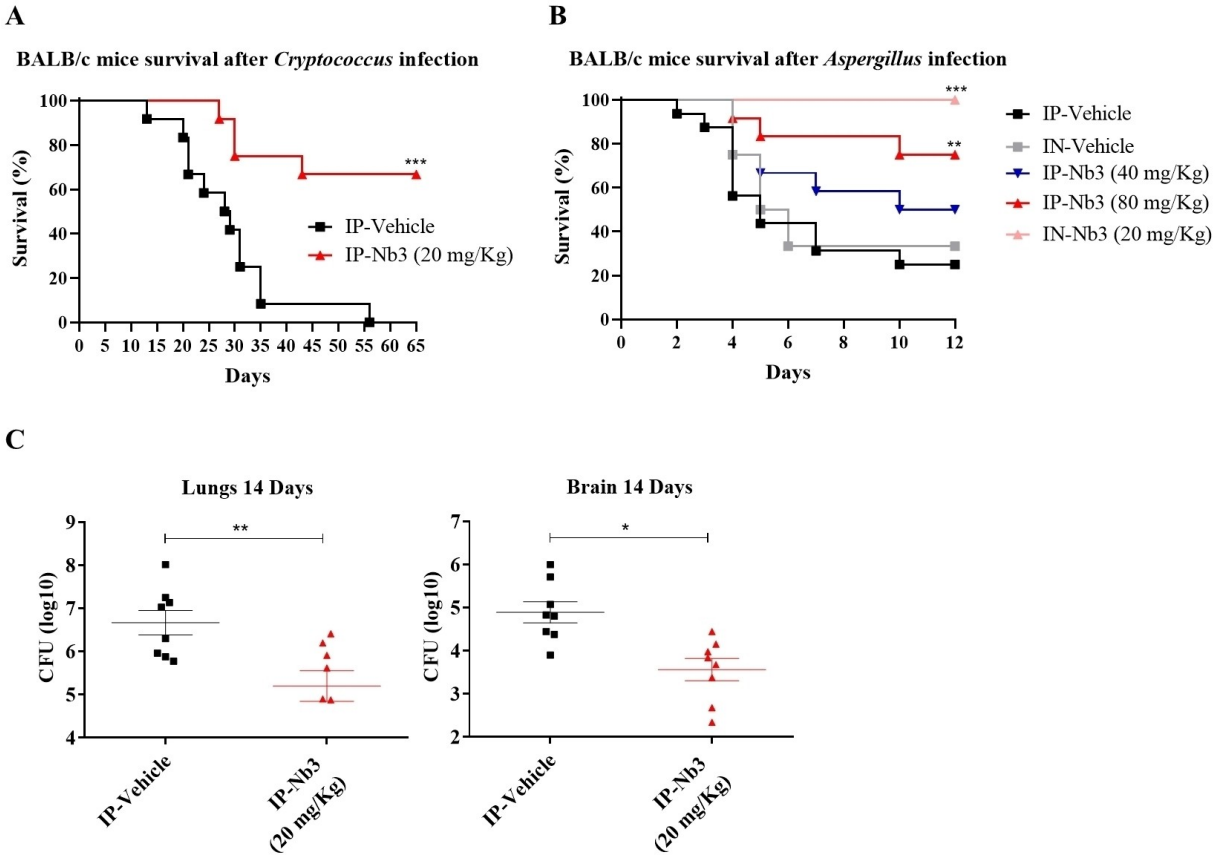

Figure 7. Prophylactic efficacy of Nb3 in mouse models of *C. deneoformans* and *A. fumigatus* infection. Survival of BALB/c female mice infected intranasally (IN) with 2.5×10^7 CFU of *C. deneoformans* (A; $n=24$) or 10^6 CFU of *A. fumigatus* (B; $n=64$) in 20 µL of PBS and treated prophylactically with PBS (vehicle) or Nb3 administered IP (intraperitoneally; A and B) or IN (B) as indicated. Results were analysed by mantel-Cox test: $^{**}p<0.01$ and $^{***}p<0.001$. C) CFU counts of mouse lung and brain homogenates infected with *C. deneoformans* and treated prophylactically IP were determined 14 days after infection. Results were analysed by unpaired t-test comparing CFU counts of lungs ($^{**}p<0.01$) and brains ($^{*}p<0.05$) of mice treated IP with PBS or Nb3.

the only effective oral treatment for diseases like invasive aspergillosis, are facing resistance.[31] Targeting cell wall proteins as drug targets has barely been exploited, yet they constitute a niche for developing new drugs to combat human fungal diseases. Here, β-1,3-glucanosyltransferases have been successfully validated as promising drug targets against fungal infections. It has also been demonstrated that the connection between enzymes involved in synthesis (e.g., β-1,3-GS) and β-1,3-glucan remodeling can be leveraged for combinatorial antifungal treatments. Additionally, we have highlighted the potential of Nbs, particularly Nb3, as valuable drugs for the frontline treatment of invasive fungal diseases. Furthermore, our research offers mechanistic and structural insights that enhance our understanding of how Nb3 and Nb4 inhibit β-1,3-glucanosyltransferases. Nb3 competes with β-1,3-glucan for binding to the Gel4 catalytic domain, while Nb4 likely competes with this polysaccharide for binding to the Gel4 CBM43 domain.

Interestingly, while Nb2 and Nb4 can inhibit Gel4 in vitro, they do not inhibit *A. fumigatus* growth, likely due to the inaccessible location of the CBM43 domain next to the GPI membrane anchor. In contrast, Nb3 seems to interact with the catalytic domain without accessibility issues and can disrupt cell wall integrity by affecting the enzyme activity. Our studies confirm that Nb3 antifungal effect is specific, not a result of nonspecific binding or altering other pathways. This specificity and in vitro efficacy offer insights into the mechanisms of β-1,3-glucanosyltransferases, informing the development of new antifungal drugs.

We have shown that Nb3 displays potent antifungal effects in both preventative and treatment contexts, working effectively through various delivery methods, including intranasal application. Nb3 targets Gel4/*Cn*Gel specifically, showing strong antifungal activity against *A. fumigatus* and superior activity against *C. deneoformans* compared to *C. neoformans*, due likely to differences in the importance of β-1,3-glucan remodeling and composition of the cell wall structure between serotypes. Actually, cell walls of *C. neoformans* are thicker and more resistant to enzymatic and physical disruption than those of *C. deneoformans*.[32]

VCZ, FCZ, and their analogs are current top choices for treating invasive aspergillosis and cryptococcosis, while AMB is a primary treatment for the initial weeks of cryptococcosis and a gold standard for invasive aspergillosis.[33] However, our data indicate that combining VCZ, FCZ, or AMB with Nb3 does not result in synergistic

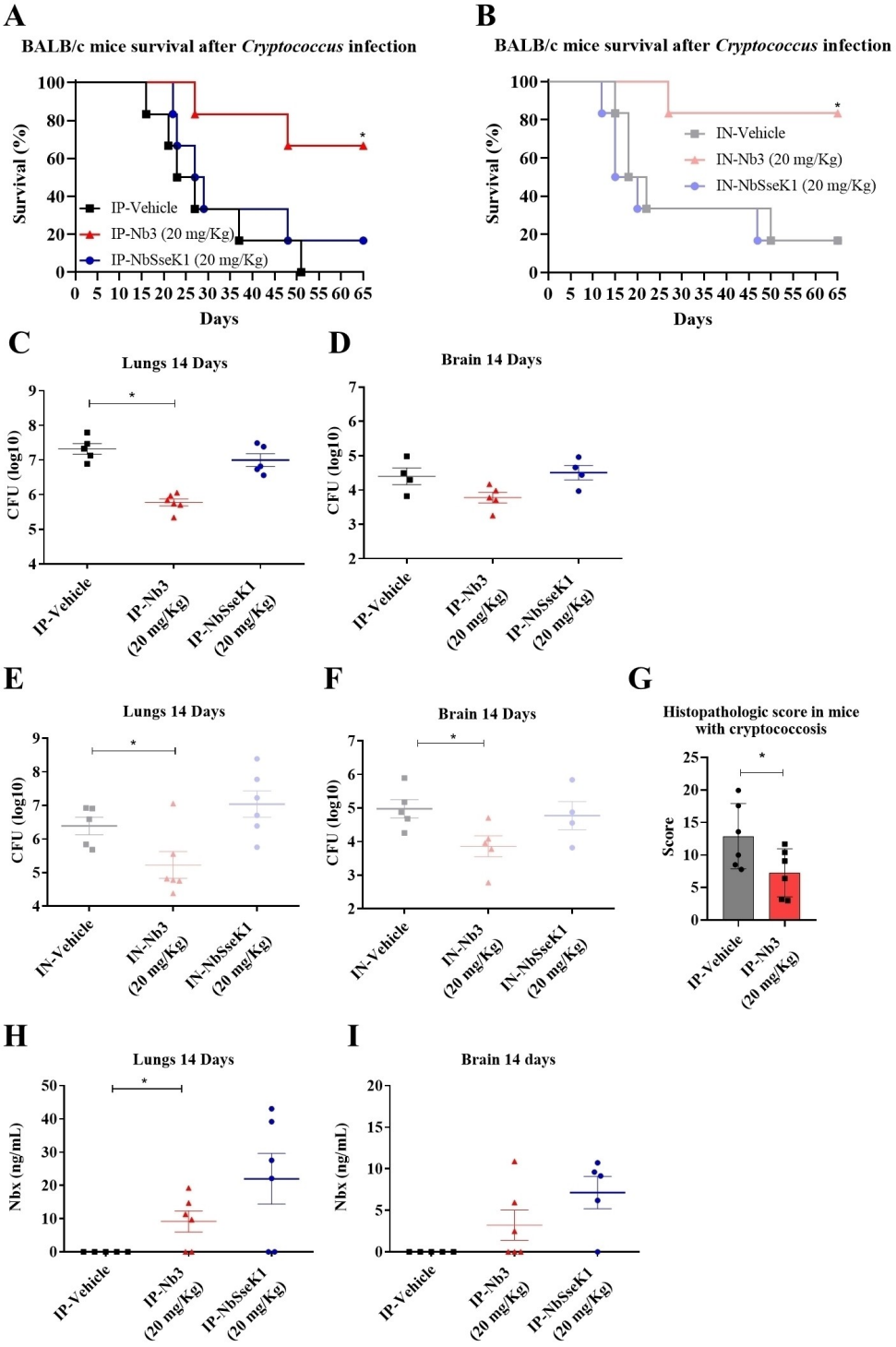

Figure 8. Therapeutic efficacy of Nb3 in mouse models of *C. deneoformans*infection. A,B) Survival of BALB/c mice infected with *C. deneoformans* treated therapeutically IP (A; $n=18$) or IN (B; $n=18$) with PBS (vehicle), Nb3, or NbSseK1, 24 h after infection, three times per week throughout the experiment. Results were analysed by mantel-Cox test:*$p<0.05$. C,D) CFU counts of mouse lung and brain homogenates infected with *C. deneoformans* ($n=18$) and therapeutically treated with intraperitoneal vehicle, Nb3 or NbSseK1 were determined after 14 days of infection. Results were analysed by unpaired t-test: *$p<0.05$. E,F) CFU counts of mouse lung and brain homogenates infected with *C. deneoformans* ($n=18$) and therapeutically treated with intranasal vehicle, Nb3 or NbSseK1 were determined after 14 days of infection. Results were analysed by unpaired t-test: *$p<0.05$. G) Histopathologic score obtained from hematoxylin-eosin (HE) staining of lung sections after 14 days of infection with *C. deneoformans* in mice ($n=12$) IP treated with PBS or Nb3 (20 mg/kg). Results were analysed by 2-way ANNOVA with Bonferroni post-test: *$p<0.05$. H,I) His-tag ELISA analysis of the presence of Nbs after IP administration in the lungs and brains of mice ($n=17$) infected with *C. deneoformans.* Results were analysed by unpaired t-test: *$p<0.05$.

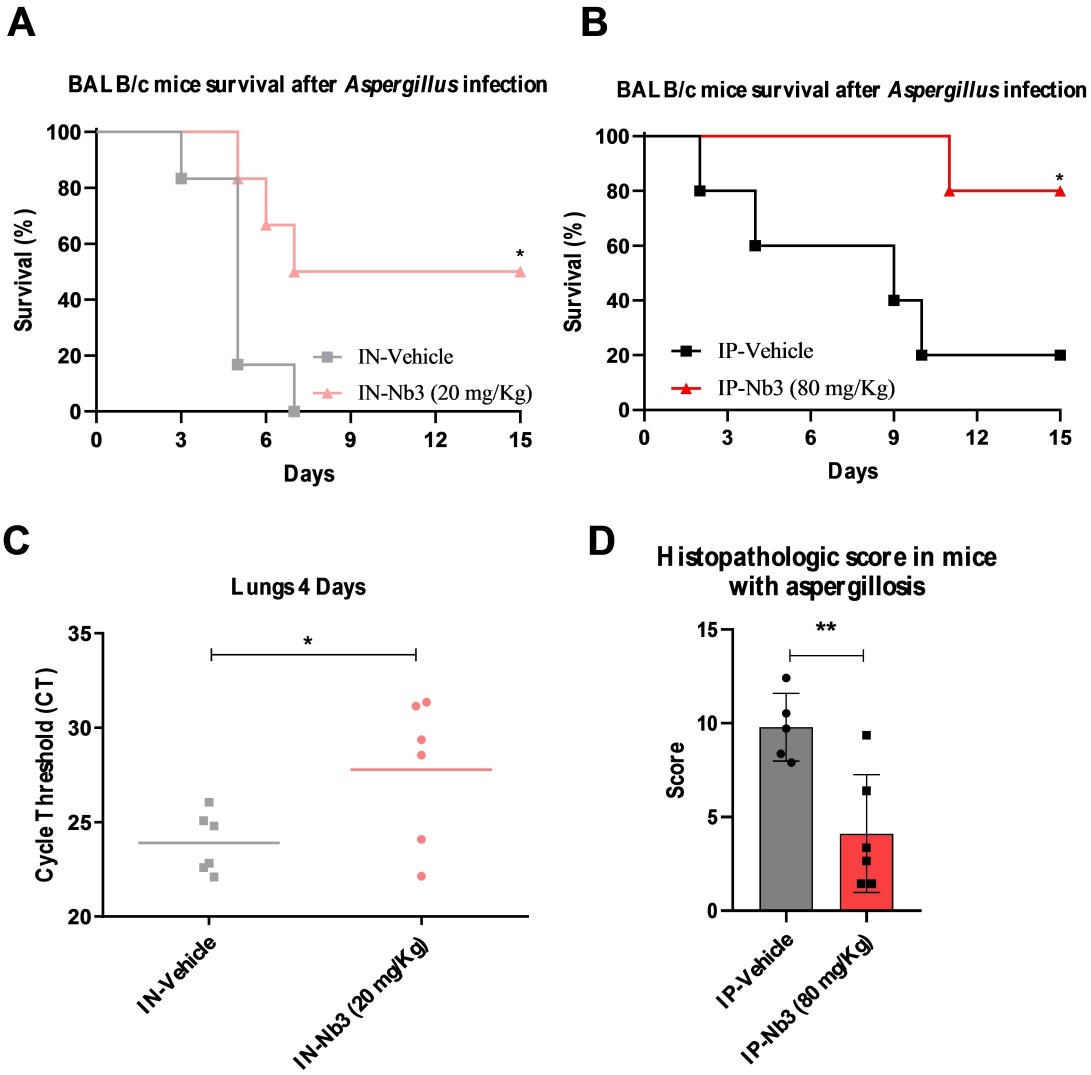

Figure 9. Therapeutic efficacy of Nb3 in a mouse model of *A. fumigatus* infection. A,B) Survival of BALB/c mice infected IN with *A. fumigatus* and treated therapeutically IN (A; $n=12$) or IP (B; $n=12$) with PBS (vehicle) or Nb3 daily 24 h after the infection during a week. Results were analysed by Mantel-Cox test: *$p<0.05$. C) Lung homogenates were prepared from *A. fumigatus* infected mice ($n=12$) treated therapeutically IN with PBS or Nb3 and fungal burden was determined by real-time PCR. Results were analysed by unpaired t-test: *$p<0.05$. D) Histopathologic score obtained from HE staining of lung sections after 3 days of infection with *A. fumigatus* in mice ($n=12$) IP treated with PBS or Nb3. Results were analysed by unpaired t-test: **$p<0.01$.

effects, except for the AMB–Nb3 combination and, interestingly Nb3-Nb4 combinations in *A. fumigatus*. Although experimental evidence is lacking to explain this synergy, it can be speculated that Nb3 binding to Gel4/*Cn*Gel may induce a conformational change, potentially exposing the CBM domain that might be hidden due to its proximity to the plasma membrane, thus enabling Nb4 interaction. Regarding AMB, disruption of cell wall integrity by Nb3 might increase its permeability to AMB, reaching higher concentrations on the fungal cell membrane where AMB binds to sterols as previously suggested for the combination of AMB and echinocandins.[34] Either way, our finding suggests that Nb3 could help reduce the drug associated toxicity in treating invasive aspergillosis and cryptococcosis.

In summary, our findings demonstrate Nb3 effectiveness in combating *A. fumigatus* and *C. deneoformans* infections and provide insights into its mechanism of action. Overall, our findings are important as they present a novel immunotherapy for invasive fungal diseases, paving the way for developing new Nbs targeting vital fungal components and innovative treatments for these life-threatening diseases.

Supporting Information

Methods, Figures S1 to S21, Tables S1 to S6

Author Contributions

R.H.-G., J.P., and E.G. conceived the project, secured funding, planned, and co-authored the manuscript with input from all listed authors. S.R.-H., M.A., and E.D. conducted the majority of the in vitro and in vivo experiments. J.M.-L., J.C.-L., A.M.G.-R., and D.S.-N. carried out the ITC experiments, purified all proteins, and facilitated the crystallization of both complexes. R.H.-G. determined and analysed both crystal structures. A.B.S., Y.P., and J.A. handled the purification of *Cn*Gels and executed the kinetic experiments. V.F. synthesised the acceptor substrates for the kinetic studies. C.V. and S.M. generated the nanobodies targeting Gel4. I.G.-B. and O.Z. were instrumental in creating the knockouts for *CnGels*. C.d.A. performed the immunohistochemistry experiments.

Acknowledgements

We thank the Diamond Light Source (Oxford, UK) synchrotron beamlines I24 and I04-1 (experiment numbers mx20229-2 and mx20229-1, respectively). We thank ARAID, CIBERINFEC (CB21-13-0087 and CB21/13/00105, IS Carlos III, Spain), the Slovak Grant Agency for Science (VEGA), Ministry of Science, Innovation and Universities and Agencia Estatal de Investigación, Spain (BIO2016-79289-P, PID2019-105223GB-I00/AEI/10.13039/501100011033, PID2022-136888NB-I00/AEI/10.13039/501100011033, CTQ2013-44367-C2-2-P, BFU2016-75633-P, PID2019-105451GB-I00, SAF2017-83120-C2-1-R, PID2020-113963RB-I00, PID2020-114546RB-I00 and PID2022-136362NB-I00), Comunidad Autónoma de Madrid (CAM) (S2017/BMD3691-InGEMICS-CM), ASPANOA and Gobierno de Aragón (B29_17R, E34_R17, LMP58_18 and LMP139_21) with FEDER (2014-2020) funds for 'Building Europe from Aragón' for financial support. The research leading to these results has also received funding from the FP7 (2007-2013) under BioStruct-X (grant agreement No. 283570 and BIOSTRUCTX_5186). M.A. was supported by a post-doctoral fellowship "Juan de la Cierva-formación" (FJCI-2017-31629), J.C.-L. and I.G.-B. were supported by FPI fellowships from Ministerio de Ciencia e Innovación, and J.M.-L. and S.R. by a predoctoral fellowship from Gobierno de Aragón. We thank a crowdfunding initiative through the platform Precipita (Nanofungi) for funding support. We would also like to acknowledge Laura Popolo for providing us with Gas1, Phr1 and Phr2, and Genomics and Proteomics Units at the UCM for assistance. We would also like to acknowledge James Kronstad (British Columbia University, Vancouver, Canada) for the gift of the acapsular cap60 strain, and Arturo Casadevall (John Hopkins University, Baltimore, MA, USA), for the gift of the 18B7 mAb.

Conflict of Interest

The authors declare the following competing financial interest(s): J.P., E.M.G., S.M., J.A. and R.H.-G. have filed a patent application (International Application No. EP20383097) related to this project.

Data Availability Statement

Atomic coordinate files and structure factors have been deposited in the Protein DataBank (PDB) with accession codes 8PE2 (dGel4-Nb3 complex) and 8PE1 (dGel4-Nb4 complex). Data collection and refinement statistics are presented in Table S2.

Keywords: Glucanosyltransferases · transglycosylases · cell wall · nanobodies · invasive fungal infections

[1] D. W. Denning, *Lancet Infect. Dis.* **2024**.
[2] G. D. Brown, D. W. Denning, N. A. Gow, S. M. Levitz, M. G. Netea, T. C. White, *Sci. Transl. Med.* **2012**, *4*, 165rv113.
[3] T. Roemer, D. J. Krysan, *Cold Spring Harbor Perspect. Med.* **2014**, *4*.
[4] a) R. A. Barnes, N. A. Gow, D. W. Denning, R. C. May, K. Haynes, M. British Society of Medical, *Lancet* **2014**, *384*, 1427; b) A. H. Fairlamb, N. A. Gow, K. R. Matthews, A. P. Waters, *Nat. Microbiol.* **2016**, *1*, 16092.
[5] Y. Lee, H. Bao, S. Viramgama, *Am. J. Health-Syst. Pharm.* **2018**, *75*, 1013–1017.
[6] P. K. Mukherjee, D. Sheehan, L. Puzniak, H. Schlamm, M. A. Ghannoum, *J. Chemother.* **2011**, *23*, 319–325.
[7] a) V. Aimanianda, C. Simenel, C. Garnaud, C. Clavaud, R. Tada, L. Barbin, I. Mouyna, C. Heddergott, L. Popolo, Y. Ohya, M. Delepierre, J. P. Latge, *mBio* **2017**, *8*; b) I. Mouyna, T. Fontaine, M. Vai, M. Monod, W. A. Fonzi, M. Diaquin, L. Popolo, R. P. Hartland, J. P. Latge, *J. Biol. Chem.* **2000**, *275*, 14882–14889.
[8] N. A. R. Gow, J. P. Latge, C. A. Munro, *Microbiol. Spectr.* **2017**, *5*.
[9] E. Drula, M. L. Garron, S. Dogan, V. Lombard, B. Henrissat, N. Terrapon, *Nucleic Acids Res.* **2022**, *50*, D571–D577.
[10] a) A. Gastebois, T. Fontaine, J. P. Latge, I. Mouyna, *Eukaryotic Cell* **2010**, *9*, 1294–1298; b) L. Popolo, G. Degani, C. Camilloni, W. A. Fonzi, *J Fungi (Basel)* **2017**, *3*; c) E. Ragni, T. Fontaine, C. Gissi, J. P. Latge, L. Popolo, *Yeast* **2007**, *24*, 297–308.
[11] a) S. M. Saporito-Irwin, C. E. Birse, P. S. Sypherd, W. A. Fonzi, *Mol. Cell. Biol.* **1995**, *15*, 601–613; b) F. De Bernardis, F. A. Muhlschlegel, A. Cassone, W. A. Fonzi, *Infect. Immun.* **1998**, *66*, 3317–3325.
[12] a) T. Di Mambro, I. Guerriero, L. Aurisicchio, M. Magnani, E. Marra, *Front. Pharmacol.* **2019**, *10*, 80; b) S. Palliyil, M. Mawer, S. A. Alawfi, L. Fogg, T. H. Tan, G. B. De Cesare, L. A. Walker, D. M. MacCallum, A. J. Porter, C. A. Munro, *Antimicrob. Agents Chemother.* **2022**, *66*, e0195721.
[13] A. L. Matveev, V. B. Krylov, Y. A. Khlusevich, I. K. Baykov, D. V. Yashunsky, L. A. Emelyanova, Y. E. Tsvetkov, A. A. Karelin, A. V. Bardashova, S. S. W. Wong, V. Aimanianda, J. P. Latge, N. V. Tikunova, N. E. Nifantiev, *PLoS One* **2019**, *14*, e0215535.
[14] S. Steeland, R. E. Vandenbroucke, C. Libert, *Drug Discovery Today* **2016**, *21*, 1076–1113.
[15] S. Muyldermans, *Annu. Rev. Biochem.* **2013**, *82*, 775–797.
[16] J. B. Park, Y. H. Kim, Y. Yoo, J. Kim, S. H. Jun, J. W. Cho, S. El Qaidi, S. Walpole, S. Monaco, A. A. Garcia-Garcia, M. Wu, M. P. Hays, R. Hurtado-Guerrero, J. Angulo, P. R. Hardwidge, J. S. Shin, H. S. Cho, *Nat. Commun.* **2018**, *9*, 4283.

[17] M. Mazan, N. Blanco, K. Kovacova, Z. Firakova, P. Rehulka, V. Farkas, J. Arroyo, *Biochem. J.* **2013**, *455*, 307–318.
[18] R. Hurtado-Guerrero, A. W. Schuttelkopf, I. Mouyna, A. F. Ibrahim, S. Shepherd, T. Fontaine, J. P. Latge, D. M. van Aalten, *J. Biol. Chem.* **2009**, *284*, 8461–8469.
[19] L. Raich, V. Borodkin, W. Fang, J. Castro-Lopez, D. M. van Aalten, R. Hurtado-Guerrero, C. Rovira, *J. Am. Chem. Soc.* **2016**, *138*, 3325–3332.
[20] a) R. Rodriguez, M. Villalba, E. Batanero, O. Palomares, J. Quiralte, G. Salamanca, S. Sirvent, L. Castro, N. Prado, *J. Invest. Allergol. Clin. Immunol.* **2007**, *17 Suppl 1*, 4–10; b) P. Barral, C. Suarez, E. Batanero, C. Alfonso, D. Alche Jde, M. I. Rodriguez-Garcia, M. Villalba, G. Rivas, R. Rodriguez, *Biochem. J.* **2005**, *390*, 77–84.
[21] M. A. Trevino, O. Palomares, I. Castrillo, M. Villalba, R. Rodriguez, M. Rico, J. Santoro, M. Bruix, *Protein Sci.* **2008**, *17*, 371–376.
[22] J. Yockey, L. Andres, M. Carson, J. J. Ory, A. J. Reese, *mSphere* **2019**, *4*.
[23] E. Ragni, J. Calderon, U. Fascio, M. Sipiczki, W. A. Fonzi, L. Popolo, *Fungal Genet. Biol.* **2011**, *48*, 793–805.
[24] Q. Y. Yin, P. W. de Groot, H. L. Dekker, L. de Jong, F. M. Klis, C. G. de Koster, *J. Biol. Chem.* **2005**, *280*, 20894–20901.
[25] a) A. Rieder, S. H. Knutsen, S. Ballance, S. Grimmer, D. Airado-Rodriguez, *Carbohydr. Polym.* **2012**, *90*, 1564–1572; b) K. G. Jørgensen, S. Aastrup, *Carlsberg Res. Commun.* **1988**, *53*, 287.
[26] I. Arcones, C. Roncero, *Methods Mol. Biol.* **2016**, *1369*, 59–72.
[27] I. R. Banks, C. A. Specht, M. J. Donlin, K. J. Gerik, S. M. Levitz, J. K. Lodge, *Eukaryotic Cell* **2005**, *4*, 1902–1912.
[28] C. S. Ahamefule, Q. Qin, A. S. Odiba, S. Li, A. N. Moneke, J. C. Ogbonna, C. Jin, B. Wang, W. Fang, *Front. Cell. Infect. Microbiol.* **2020**, *10*, 320.
[29] a) C. Rodriguez-de la Noval, S. Ruiz Mendoza, D. de Souza Goncalves, M. da Silva Ferreira, L. Honorato, J. M. Peralta, L. Nimrichter, A. J. Guimaraes, *J Fungi (Basel)* **2020**, *6*; b) W. J. Steinbach, D. K. Benjamin Jr., S. A. Trasi, J. L. Miller, W. A. Schell, A. K. Zaas, W. M. Foster, J. R. Perfect, *Med. Mycol.* **2004**, *42*, 417–425.
[30] C. Coelho, E. Camacho, A. Salas, A. Alanio, A. Casadevall, *mSphere* **2019**, *4*.
[31] A. Bueid, S. J. Howard, C. B. Moore, M. D. Richardson, E. Harrison, P. Bowyer, D. W. Denning, *J. Antimicrob. Chemother.* **2010**, *65*, 2116–2118.
[32] A. J. Reese, A. Yoneda, J. A. Breger, A. Beauvais, H. Liu, C. L. Griffith, I. Bose, M. J. Kim, C. Skau, S. Yang, J. A. Sefko, M. Osumi, J. P. Latge, E. Mylonakis, T. L. Doering, *Mol. Microbiol.* **2007**, *63*, 1385–1398.
[33] D. Allen, D. Wilson, R. Drew, J. Perfect, *Expert Rev. Anti-Infect. Ther.* **2015**, *13*, 787–798.
[34] S. Arikan, M. Lozano-Chiu, V. Paetznick, J. H. Rex, *Antimicrob. Agents Chemother.* **2002**, *46*, 245–247.

Manuscript received: April 1, 2024
Accepted manuscript online: June 10, 2024
Version of record online: July 22, 2024